

Morphological Instability and Additive-Induced Stabilization in Electrodeposition

Mikko Haataja and David J. Srolovitz

*Princeton Materials Institute and Department of Mechanical and Aerospace Engineering, Princeton University,
Princeton, New Jersey 08544*

(Received 23 April 2002; published 4 November 2002)

Experiments show that electrodeposited (ED) films exhibit rough surfaces unless the electrochemical bath contains small quantities of molecular “additive” species. We develop a model for ED with additives which shows the suppression of the morphological instability by preferential additive accumulation near surface protrusions due to complex formation and additive codeposition, and subsequent growth site blocking. Linearly stable growth can be achieved over a wide range of deposition flux at sufficiently large additive bulk concentration. We predict the growth conditions necessary for level surfaces, in good agreement with experiments.

DOI: 10.1103/PhysRevLett.89.215509

PACS numbers: 81.10.Aj, 81.10.Dn, 81.15.Pq

Electrodeposition (ED) is widely employed in the deposition of pure metals and alloys for interconnects in microelectronics, as magnetic media in magnetic recording devices, to fabricate high aspect ratio micromachines, and for plating inexpensive watches [1,2]. Film growth by ED employs an external current that drives metal ions (cations) in an aqueous ionic solution (“bath”) onto the cathode. In most applications, a smooth film surface is required. However, morphological instabilities during deposition commonly produce poor quality films with rough surfaces [3–5]. Morphologies ranging from the preferred flat topography to dendritic to diffusion-limited-aggregation-like have been observed, depending on experimental conditions. The key to growing high-quality films lies, in part, in suppression of a naturally occurring instability.

Years of experimental empiricism have shown [6,7] that film properties can be effectively controlled by introducing small quantities of molecular additive species to the electrochemical bath. In addition to controlling the large-scale roughness (“leveling”), additives have been used to control crystallographic texture and grain size of the film. For example, Schilardi *et al.* [5] showed that adding sufficient thiourea to a copper ED bath leads to a marked decrease in the surface roughness and near suppression of the growth instability.

Although some progress has been made in recent years, the development and application of additives remains largely an art, based upon enlightened empiricism. This is in contrast with the emerging understanding of the role of additives in semiconductor growth (see [8] and references therein). In ED, additives are readily adsorbed onto the growing surface and often incorporated into the deposit [7]. Several models for the interaction between additives and the depositing cations have been proposed, such as surface blocking, complex formation, ion bridging, and changes in the electrostatic fields near the surface [6,7,9]. According to the blocking model, additive molecules adsorbed at the surface physically block potential growth sites. If the additives form a complex with the

cations in the bath, they may be carried to the surface by the drifting cations. As will be demonstrated below, this effect can play an important role in the growth front stabilization. In ion bridging, the additive, which bonds both to the surface and the cation, mediates the electron transfer. Finally, as the deposition kinetics are sensitive to the electric field near the surface (see below), foreign species which modify it will modify the deposition rate.

In this Letter, we explore the origin of the surface instability during ED and develop a predictive model for the mechanisms by which the additives suppress this instability. This analysis is performed within the framework of linear stability theory and leads to the classical Mullins-Sekerka (MS) instability [10] in the absence of additives [4,11]. Our physically based model shows that additives which readily adsorb onto the surface and have a strong tendency to complex with the cations reduce the driving force for the instability. For deposition fluxes below a critical one, we demonstrate that the planar ED growth front becomes linearly stable above a critical additive bulk concentration. For larger fluxes, however, the additives are incapable of leveling the surface. Finally, we construct a map that relates growth conditions and materials parameters to the morphology of the ED grown films. The resultant predictions are in good correspondence with experimental observations of the effects of additives on ED surface morphologies [5,7].

We begin by writing a continuity equation for the concentration of each species in the laboratory frame: $(\partial C_i / \partial t) + \nabla \cdot \vec{j}_i = 0$, where $i = C, A, XC, XA, I$ for the cations, anions, excess cations, excess anions, and additives, respectively. Excess ions are charged particles which do not deposit but are added to the bath to reduce convective transport and to keep the charged boundary layer compact [12]. We first consider a bath without additives. In this case, the ionic fluxes have contributions from the entropy of mixing and the drift in the local electric field: $\vec{j}_i = -D_i \nabla C_i - (q_i e D_i / k_B T) C_i \nabla \phi$, where D_i denotes the diffusivity, and $q_i e$ is the charge on the ionic species in the solution. Furthermore, the coupling

between the ions is provided by the electric potential ϕ , which satisfies $\nabla^2 \phi = -\frac{1}{\epsilon} \sum_i q_i C_i(\vec{r})$, where $\hat{\epsilon}$ denotes the permittivity of the solution. We assume a constant $\hat{\epsilon}$, since the stability properties of the surface are only weakly dependent on its spatial dependence [13].

System dimensions for our two-dimensional (2D) setup are $L_x \times L_z = W \times \delta$, where W denotes the linear dimension (width) of the planar surface and δ is an effective diffusion distance, beyond which all C_i are constant. We employ periodic boundary conditions in the x direction, and the boundary conditions in the z direction become $C_C(x, \delta) = C_A(x, \delta) = C_0$, $C_{XC}(x, \delta) = C_{XA}(x, \delta) = C_1$, and $\phi(x, \delta) = 0$. At the cathode surface, $\phi(x, 0) = V_{\text{ext}}$, and the ion fluxes $i = (A, XC, XA)$ vanish: $j_i = \vec{j}_i \cdot \vec{n} = 0$, where \vec{n} is the surface normal. The magnitude of the cation flux onto the growing surface j_C is given by the Butler-Volmer (BV) equation

$$j_C = j_0(C_C e^{\alpha_1 F \eta / RT} / C_0 - e^{-\alpha_2 F \eta / RT}), \quad (1)$$

where F and R are Faraday's and the gas constant, and (α_1, α_2) denote the so-called symmetry factors related to the potential barrier for cation reduction [1]. The overpotential η is given by $\eta = V_{\text{eq}} - V_{\text{ext}} + RT/\ln$

$F \ln(C_C/C_C^{\text{eq}}) + \Omega \gamma \kappa / F q_C$ [11]. The equilibrium potential of the metal-solution interface is V_{eq} , and varying the external electrode potential V_{ext} leads to either deposition ($\eta > 0$) or dissolution ($\eta < 0$). The second term accounts for the concentration dependence of V_{eq} , and the last term describes the effects of curvature κ and surface tension γ , i.e., the Gibbs-Thomson effect. The quantity $q_C e j_0$ denotes the exchange current density, and Ω denotes the atomic volume of the metal. The local growth velocity v_n follows simply from $v_n = \Omega j_C$. Although this analysis is in 2D, the main results of the linear stability analysis are unchanged in 3D. Modifications due to, e.g., anisotropic surface tension, can be incorporated within our formalism, but provide little new insight.

It is straightforward [13] to find the steady-state solution in this model upon recognizing [14] that the presence of mobile charges gives rise to a charged boundary layer beyond which the electric field is screened in equilibrium. The dimensionless width of the charged boundary layer is a small parameter, $\epsilon \equiv \sqrt{\hat{\epsilon} V_{\text{eq}} / (C_0 + C_1) e} / \delta = \lambda_D / \delta$, where λ_D denotes the Debye screening length [12] (typically $\lambda_D \sim 10$ nm, $\delta \sim 1$ cm, and $\epsilon \sim 10^{-6}$). We perform a standard boundary layer analysis (see, e.g., [15]) using $\epsilon \ll 1$ as an expansion parameter, and obtain [16]

$$\phi(z; \epsilon) = -\left[\frac{1}{\alpha_1^C \phi^*} \ln\left(1 - \frac{j}{2 + 2C_1}\right) - 1 \right] \frac{4}{\alpha_1^C} \tanh^{-1}\left(e^{-\sqrt{2\alpha_1^C} z / \epsilon} \tanh \frac{\alpha_1^C \phi^*}{4} \right) + \frac{1}{\alpha_1^C} \ln\left(1 - \frac{j}{2 + 2C_1} + \frac{jz}{2 + 2C_1}\right), \quad (2)$$

where $j = (j_C \delta) / (D_C C_0)$ denotes the dimensionless flux, $\phi^* = V_{\text{ext}} / V_{\text{eq}}$, $\alpha_1^C \equiv q e V_{\text{eq}} / k_B T$, the coordinate z has been normalized by δ , and all concentrations have been normalized by C_0 . The cation concentration is determined from $C_C = (1 + C_1) \exp(\alpha_1^C \phi) - C_1 \exp(-\alpha_1^C \phi) - (1 + C_1) \epsilon^2 d^2 \phi / dz^2$. Figure 1 shows the spatial variation of the potential ϕ for several values of C_1 . Note the presence of a boundary layer adjacent to the electrode and that ϕ tends to zero with increasing excess ion concentration ($C_1 \rightarrow \infty$ implies a "fully supported" electrolyte). When C_1 is small, the electric field is nonzero within the electrolyte. In the limit $C_1 \gg 1$, $\phi = \mathcal{O}(1/C_1)$ and $C_C = 1 - j + jz + \mathcal{O}(1/C_1)$. In this case, only cation diffusion contributes to the flux, and drift effects in the bulk are negligible. For simplicity, we focus on the $C_1 \rightarrow \infty$ case in this Letter (see [13] for the general case). Finally, the cation flux j can be expressed in terms of V_{ext} through the BV relation [Eq. (1)].

The short-time evolution of the surface morphology can be understood by considering a small perturbation to the planar interface. Since $\nabla C_C \cdot \hat{n} = j > 0$, C_C is larger (smaller) near protrusions (depressions) than near the flat surface. In the absence of surface tension, an increase in C_C leads to a larger flux via the BV equation [cf. Eq. (1)]. The larger flux leads to an increase in v_n and hence faster protrusion growth. This positive feedback leads to unstable growth of the perturbations. Surface tension can restrain this instability at short wavelengths, leaving it only

at large wavelengths in a manner analogous to the MS instability of a solidification front [10].

The more formal linear stability analysis proceeds as follows. The surface perturbation $\delta \xi = \delta \hat{\xi} e^{ikx + \omega(k)t}$ implies a variation in the dimensionless normal growth velocity $\delta v = \omega(k) \delta \xi = \Omega C_0 \delta j \equiv \Omega' \delta j$, where all length scales have been normalized by δ . The perturbed cation concentration field $\delta C_C = \delta \hat{C}_C e^{ikx - kz + \omega(k)t}$ can be found by applying the BV equation at the perturbed interface and linearizing it in $\delta \xi \ll 1$ to yield δj , and thus $\omega(k)$. In the limit $k \gg 1$ and $F \eta / RT \gg 1$ (appropriate for growth), we obtain [13]

$$\frac{\omega(k)}{\Omega'} = \frac{jk \left[\frac{j(1+\alpha_1)}{(1-j)} - \hat{\gamma} \alpha_1 k^2 \right]}{\left[\frac{j(1+\alpha_1)}{(1-j)} + k \right]}, \quad (3)$$

with the dimensionless surface tension $\hat{\gamma} \equiv \Omega \gamma / RT \delta$. In the limit $k \ll j / (1 - j)$, Eq. (3) reduces to the standard MS relation $\omega(k) / \Omega' \approx jk - (1 - j) \hat{\gamma} \alpha_1 k^3 / (1 + \alpha_1)$ [4,10,11], while in the opposite limit, $\omega(k) / \Omega' \approx j^2 (1 + \alpha_1) - j \hat{\gamma} \alpha_1 k^2$. From Eq. (3) we obtain $\omega(k) > 0$ for $0 < k < k_0 = \sqrt{(1 + \alpha_1) j / [\alpha_1 \hat{\gamma} (1 - j)]}$, implying exponentially fast growth of perturbations of these wave numbers. The fastest growing wave number $k_{\text{max}} = k_0 / \sqrt{3 + [2(1 - j) / j(1 + \alpha_1)]}$ with growth rate $\omega(k_{\text{max}}) \equiv \omega_{\text{max}}$ dominates the early-time behavior and

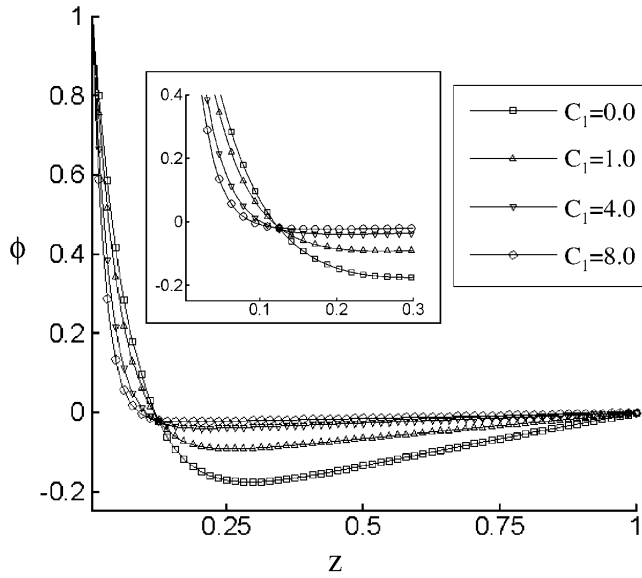


FIG. 1. Electric potential ϕ for $j = 0.5$ and several excess ion bulk concentration C_1 , corresponding to $\epsilon \approx 0.1$. Note the rapid variation of the potential in the vicinity of the electrode ($z = 0$) and the effective screening of the electric field in the bulk by the excess electrolyte. Inset: A close-up of the charged boundary layer.

thus determines the characteristic scale of the roughness. Physically, the presence of finite k_0 is due to surface tension which suppresses the instability on scales $\ell < \ell_s \equiv 2\pi/k_0$, where ℓ_s denotes the stabilization length. Since the presence of unstable modes is due to a finite external current j , an increase in j implies a concomitant increase in k_{\max} , making the surface rough on shorter scales. For example, employing the current density $J = 200$ A/m² and cation bulk concentration $C_0 = 0.6M$ from Ref. [5], and employing the reasonable values $D_C \approx 10^{-9}$ m²/s, $\gamma \approx 1.6$ J/m², we obtain $\delta \approx 4 \times 10^{-4}$ m, and $2\pi/k_{\max} \approx 0.07$ mm for the lateral scale of the roughness, in very good correspondence with the experimental result of 0.05 mm in Ref. [5].

When additives are introduced into the bath, we must account for their (dimensionless) flux: $\vec{j}_I = -\alpha_1^I \nabla C_I + \alpha_4^I C_I \nabla C_C$, where $\alpha_1^I \equiv D_I/D_C$ and $\alpha_4^I \equiv D_I \beta_C C_0 / D_C k_B T$. The last term in the flux arises from the interactions between the additives and the cations, which we describe using a phenomenological interaction free energy $F_{\text{int}} = -\beta_C \int d\vec{r} C_I(\vec{r}) C_C(\vec{r})$ [13]. This simple expression accounts for complex formation, with a dimensionless strength described by $Y \equiv \beta_C C_0 / (k_B T) = \ln K_c$, where K_c denotes the equilibrium constant for complex formation. The additive concentration is uniform beyond the effective diffusion distance $C_I(x, \delta) = C_I^\infty$. We incorporate the effect of additives in blocking potential surface growth sites by adopting a modified BV equation for the local cation flux j_C which satisfies $j_C = j_0(1 - \theta_I)(C_C e^{\alpha_1 F \eta / RT} / C_0 - e^{-\alpha_2 F \eta / RT})$, where θ_I denotes the local additive surface coverage [9]. We assume

that θ_I follows a simple Langmuir isotherm $\theta_I = KC_I / (1 + KC_I)$, where K denotes the equilibrium constant for surface segregation. Finally, motivated by experimental observations [7], we allow some of the additives to be incorporated into the growing film at a rate proportional to the cation flux: $\vec{j}_I \cdot \vec{n} = -\chi C_I^\infty j$ [17]. $\chi = 1$ implies that cations and additives are incorporated in proportions given by their bulk concentrations.

Physically, the additives occupy surface sites where cations can attach, thus slowing growth. Therefore, if protrusions collect more additives than depressions, they will grow more slowly, hence favoring the growth of smooth surfaces [1,5]. Increased additive concentrations occur where the additive flux to the surface is greatest. This flux is controlled by both additive-cation complexing (represented by Y), since cations are driven to the growth front, and by additive codeposition (represented by χ), which gives rise to an additive concentration gradient. This picture is consistent with a linear stability analysis, which shows that $\omega(k)$ now becomes [13]

$$\frac{\omega(k)}{\Omega'} = \frac{jk \left[\frac{j_{\text{eff}}(1+\alpha_1)}{(1-j_{\text{eff}})} - \hat{\gamma} \alpha_1 k^2 \right]}{\left[\frac{j(1+\alpha_1)}{(1-j)} - j\Gamma Y(1 - \chi j/\alpha_1^I) + k \right]}, \quad (4)$$

where the effective current $j_{\text{eff}}(1 + \alpha_1)/(1 - j_{\text{eff}}) \equiv j(1 + \alpha_1)/(1 - j) - \Gamma(jY + \chi j/\alpha_1^I - j^2 \chi Y/\alpha_1^I)$ and the additive effects are conveniently expressed by Γ as

$$\Gamma \equiv \frac{KC_I^\infty e^{Y(1-j)}}{1 + KC_I^\infty e^{Y(1-j)}(1 - \chi j/\alpha_1^I)}. \quad (5)$$

This equation has a very appealing physical interpretation. Since j_{eff} is always less than j , the instability is weakened by the presence of the additives. In Fig. 2 we plot $\omega(k)$ vs k for a fixed cation deposition flux j and several additive concentrations C_I^∞ . Note that increasing C_I^∞ leads to reduced k_{\max} and $\omega(k)$. Thus, for the same external conditions, increasing the additive concentration

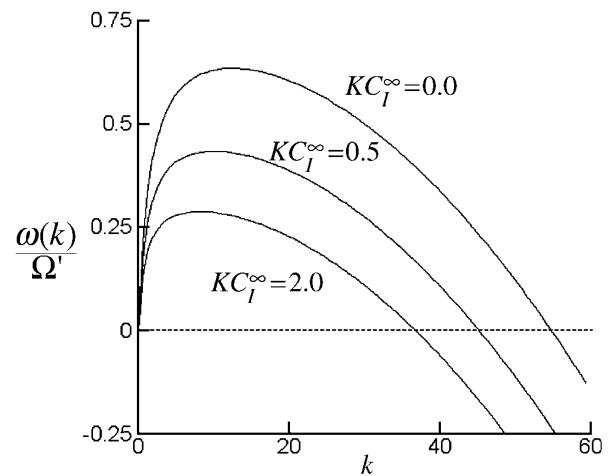


FIG. 2. Linear dispersion relation $\omega(k)/\Omega'$ vs k for $j = 0.5$, $Y = 1.5$, $\chi = 0.5$, $\alpha_1 = 0.5$, and $\hat{\gamma} = 0.001$ and several values of KC_I^∞ . Note that increasing KC_I^∞ increases the range of surface stability.

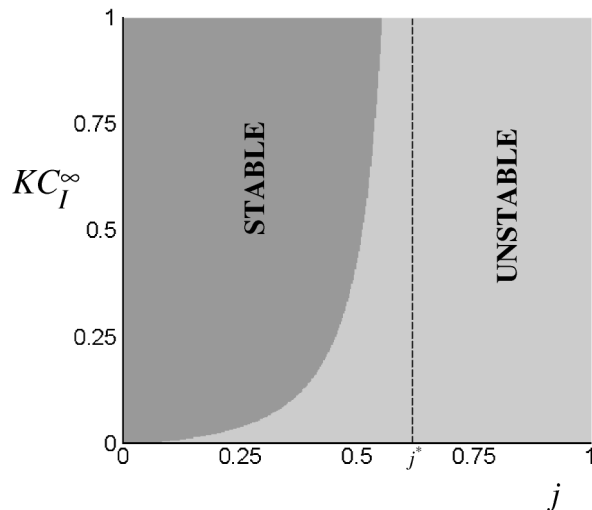


FIG. 3. Stability map. For a fixed deposition flux $j < j^*$, linearly stable growth is achieved for sufficiently large values of KC_I^∞ .

increases the range of surface stability. Equation (4) also shows that increasing the degree of additive codeposition ($\chi > 0$), the equilibrium additive surface concentration (represented by K) and the degree of coupling Y between additives and cations all enhance stability, consistent with experimental observations [7]. For example, upon employing the reasonable values $K = 10^6$, $\alpha_1^I = 1$, and $\chi = 0.5$, and experimentally determined value $0.8 < Y < 1.5$ [18], appropriate for thiourea-cupric complexes, and $C_I^\infty = 0.025$ mM, we obtain $0.1 \text{ mm} < \ell_s < 0.2 \text{ mm}$, in reasonable agreement with the experimental result of $\ell_s \sim 0.5 \text{ mm}$ in Ref. [5].

It is noteworthy that an increase in Y can compensate for a decrease in the additive codeposition rate χ ; this observation is key in cases where additive codeposition must be avoided. We also note that experiments suggest a correlation between the stabilizing effect of the additives and their dipole moment [7]. We attribute this correlation to the strong electrostatic interaction between dipolar additives and the inhomogeneous electric field near the growth front, which gives rise to an effectively larger K and thus promotes stability [13].

These results can be used to choose deposition conditions corresponding to the maximum film growth rate for which the surface remains smooth over the requisite length scale, W . To this end, we require that all perturbation modes with wavelengths smaller than W decay: $\omega(k) < 0$ for $k \geq 2\pi/W$. In order to guide the experiment, we express the stability conditions in terms of the experimentally accessible parameters, cation flux j and additive concentration C_I^∞ . In Fig. 3, we construct a stability map for the following realistic growth conditions $Y = 4.0$, $W = 1.0$, $\chi = 0.0$, $\hat{\gamma} = 0.001$, and $\alpha_1 = 0.5$. Such a map conveniently displays the full range of stable and unstable growth conditions. While introducing

additives can dramatically increase the deposition currents that can be used, there exists a critical current $j^* \approx 1 - (1 + \alpha_1)/Y$ above which the additives are incapable of leveling the surface. This can be understood by incorporating the blocking effect into an effective overpotential $\eta_{\text{eff}} \equiv \eta + (RT/F\alpha_1) \ln(1 - \theta_I)$, obtained from the modified BV equation. Since a very large η_{eff} is required to produce large deposition fluxes, this implies that $\eta \gg (RT/F\alpha_1) \ln(1 - \theta_I)$. Thus, the additives are incapable of stabilizing the smooth surface.

We thank Dr. A. Bocarsly, Dr. C. Battaile, and Dr. J. Hamilton for fruitful discussions, and Sandia National Laboratories for financial support.

- [1] M. Paunovic and M. Schlesinger, *Fundamentals of Electrochemical Deposition* (Wiley, New York, 1998).
- [2] W. Bacher, W. Menz, and J. Mohr, *IEEE Trans. Ind. Electron.* **42**, 431 (1995).
- [3] F. Argoul, A. Arnedo, G. Grasseau, and H.L. Swinney, *Phys. Rev. Lett.* **61**, 2558 (1988); D. Barkey, F. Oberholtzer, and Q. Wu, *ibid.* **75**, 2980 (1995).
- [4] G. L. M. K. S. Kahanda, X.-q. Zou, R. Farrell, and P.-o. Wong, *Phys. Rev. Lett.* **68**, 3741 (1992); J. M. Pastor and M. A. Rubio, *ibid.* **76**, 1848 (1996).
- [5] P. L. Schilardi, O. Azzoni, and R. C. Salvarezza, *Phys. Rev. B* **62**, 13 098 (2000).
- [6] J. W. Dini, *Electrodeposition: The Materials Science of Coatings and Substrates* (Noyes Publications, New York, 1993).
- [7] L. Oniciu and L. Muresan, *J. Appl. Electrochem.* **21**, 565 (1991); T. C. Franklin, *Surf. Technol.* **30**, 415 (1987).
- [8] D. Kandel and E. Kaxiras, *Solid State Phys.* **54**, 219 (2000).
- [9] C. Madore, M. Matlosz, and D. Landolt, *J. Electrochem. Soc.* **143**, 3927 (1996); Y. Cao, P. Taepaisitphongse, R. Chalupa, and A. C. West, *ibid.* **148**, C466 (2001).
- [10] W.W. Mullins and R. F. Sekerka, *J. Appl. Phys.* **34**, 323 (1963); **35**, 444 (1964).
- [11] M. D. Pritzker and T. Z. Fahidy, *Electrochim. Acta* **37**, 103 (1992); R. Cuerno and M. Castro, *Phys. Rev. Lett.* **87**, 236103 (2001).
- [12] K. B. Oldham and J.C. Myland, *Fundamentals of Electrochemical Science* (Academic Press, San Diego, 1994).
- [13] M. Haataja and D. J. Srolovitz (to be published).
- [14] A. Bonnefont, F. Argoul, and M. Z. Bazant, *J. Electroanal. Chem.* **500**, 52 (2001).
- [15] A. H. Nayfeh, *Introduction to Perturbation Techniques* (Wiley, New York, 1993).
- [16] For simplicity, we assume that the diffusion length $\ell_D = 2D_C/v \geq \delta$, and that $q_C = q_{XC} = q$, $q_A = q_{XA} = -q$.
- [17] This simple approximation allows us to study the effect of codeposition without a detailed description of the process itself, of which little is known in general.
- [18] C. J. Doona and D. M. Stanbury, *Inorg. Chem.* **35**, 3210 (1996), measured K_c for thiourea-cupric ion complexes, which yields $Y = \ln K_c$.